Chemical Geology 582 (2021) 120459

Contents lists available at ScienceDirect

Chemical Geology

journal homepage: www.elsevier.com/locate/chemgeo

Precise analysis of antimony isotopic composition in geochemical materials by MC-ICP-MS

Guangyi Sun [a,1], Yunjie Wu [b,1], Xinbin Feng [a,c,*], Xian Wu [a,d], Xinyu Li [a,d], Qianwen Deng [a,d], Feiyue Wang [e], Xuewu Fu [a,c]

[a] State Key Laboratory of Environmental Geochemistry, Institute of Geochemistry, Chinese Academy of Sciences, Guiyang 550081, China
[b] School of Earth Sciences, China University of Geosciences, Wuhan 430074, China
[c] Center for Excellence in Quaternary Science and Global Change, Chinese Academy of Sciences, Xian 710061, China
[d] University of Chinese Academy of Sciences, Beijing 100049, China
[e] Centre for Earth Observation Science, Department of Environment and Geography, University of Manitoba, Winnipeg, MB R3T 2N2, Canada

ARTICLE INFO

Editor: Don Porcelli

Keywords:
Antimony
Stable isotopes
Hydrothermal systems
Geochemical samples

ABSTRACT

Antimony (Sb) isotopes have been shown to be promising tracers for studying Sb cycling in the environment and its impact on ecosystem and human health. Yet precise measurements of Sb isotopic composition have been challenged by low Sb concentrations and high matrix effect and by the lack of a common reference material (zero-delta). Here we report an improved analytical scheme that is capable of high-precision measurement of Sb isotopes in environmental and geochemical samples. The method employs a two-column ion exchange set-up to remove interfering matrix elements to allow Sb isotopic measurements with low Sb (< 0.15 μg/g) and high matrix content. The instrument mass bias is corrected by combining the sample-standard bracketing method with internal normalization of cadmium. To allow for interlaboratory comparisons, a standard reference material certified for the total Sb concentration, NIST SRM 3102a, is recommended as the reference standard ("zero-delta") for Sb isotope measurements. The improved method is applied for high-precision and high-accuracy Sb isotope composition measurements in environmental and geochemical reference samples with a minimum Sb required per analysis as low as 3.0 ng. By expressing our data and previously reported literature data against the same reference standard (NIST SRM 3102a), we provide an update on isotopic compositions of various types of environmental, geological and anthropogenic materials. The improved analytical method and database aid further studies on the mechanisms of Sb isotope fractionation and its application as a tracer for the study of the sources, processes and fate of Sb in the environment.

1. Introduction

Antimony (Sb) and its compounds are listed as priority pollutants by the European Union and U.S. Environmental Protection Agency (EPA) due to their adverse effects on human health including potentially causing cancer (European Commission, 2017; US Office of the Secretary of the Department of the Interior, 2018). Since the Early Bronze Age (4000 B.C.), Sb has been used in human medicine, veterinary medicine, and cosmetics by alchemists and medical imposters (Smichowski, 2008). Its present-day use includes as a catalyst in the manufacture of polyethylene terephthalate, and as a component of brake linings, cable covering, ammunitions, bearings, and flame retardants (Dupont et al., 2016). In 2019, 1.6×10^5 metric tonnes of Sb were produced globally (Survey, 2020), with an expected interannual increase of 5.6% (Henckens et al., 2016). As a result, considerable increases of Sb concentrations have been observed in various environments, including in peat bogs and Arctic ice cores (Shotyk et al., 2005; Krachler et al., 2005; Gabrielli et al., 2020), which call for a better understanding of Sb cycling in the environment, human exposure pathways, and mitigation strategies (Smichowski, 2008; Henckens et al., 2016; He et al., 2019; Filella et al., 2002a, 2002b; Filella et al., 2007; Alvarez-Ayuso et al., 2013; Multani et al., 2016).

Antimony has two stable isotopes, ^{121}Sb and ^{123}Sb, with an average abundance of 57.2% and 42.8%, respectively, in the natural

* Corresponding author: State Key Laboratory of Environmental Geochemistry, Institute of Geochemistry, Chinese Academy of Sciences, Guiyang 550081, China.
E-mail address: fengxinbin@vip.skleg.cn (X. Feng).
[1] These authors contributed equally to this work report.

https://doi.org/10.1016/j.chemgeo.2021.120459
Received 1 February 2021; Received in revised form 20 June 2021; Accepted 23 July 2021
Available online 26 July 2021
0009-2541/© 2021 Elsevier B.V. All rights reserved.

environment (Rouxel et al., 2003). With a Multicollector-Inductively Coupled Plasma Mass Spectrometer (MC-ICPMS), Aston (1923) first reported the abundance of Sb isotopes, and then Rouxel et al. (2003) performed precise measurements of Sb isotopic compositions of seawater, mantle-derived rocks, deep-sea sediments, and hydrothermal sulfides. Their results showed a large fractionation range (up to 19.1ε) of Sb in these substances, and revealed a strong fractionation (9ε) during Sb(V) reduction to Sb(III) (Rouxel et al., 2003). Subsequently, the Sb isotope composition has been measured for stibnite and mine drainage water (Tanimizu et al., 2011), ancient glass (Lobo et al., 2012, 2013, 2014), and river waters (Resongles et al., 2015), which showed that Sb isotopes could be used as a sensitive geochemical tracer of material sources and processes, such as redox and mineralization (Wen et al., 2018).

Although various sample preparation and analysis methods for Sb isotope measurement have been recently reported (Table 1), major challenges exist when it comes to high-precision measurement (2SD < 0.4ε). As shown in Table 1, most of the pre-concentration and separation methods use thiol cotton fiber (TCF) and ion-exchange chromatography employing a cation exchange resin (e.g., Biorad AG50-X8 (Rouxel et al., 2003), Dowex AG50-X8 (Degryse et al., 2015; Lobo et al., 2012)) or an anion exchange resin (e.g., Amberlite IRA 743 (Degryse et al., 2015; Lobo et al., 2012)). These methods are often specific to sample types (e.g., glass and drainage water) with a recovery rate varying from 76 to 104%. More recently, Liu et al. (2020) developed a two-step method with AG 1-X4 and AG 50 W-X8 resin for purifying Sb for Soil and sediment samples. AG 1-X4 resin is worthy of further study for extraction of Sb from samples. Li et al. (2021) used a commercial thiol-functionalized silica to purify Sb from contaminated water (up to 30 mg/L). Unfortunately, none of the above two methods has been applied to separate Sb from complex solid samples with low Sb contents. Ferrari et al. (2021) proposed a single-step purification method by thiol-functionalized mesoporous silica powder packed in disposable cartridges connected to a peristaltic pump. Indeed, a peculiar sample matrix may lead to unexpected incomplete recovery. Sanz et al. (1990) found that Sb signal suppression related to the oxidation of Sb(III) to Sb(V) by Fe(III) at an Fe (III): Sb mass ratio greater than 22. For an Fe-rich sample (Fe:Sb > 50,000) may still need a pre-treatment by AG 50 W-X8 (cation removal) as evidenced by Rouxel et al., 2003.

With respect to isotopic measurement on MC-ICP-MS, two types of sample injection methods are used, including wet injection and hydride generation injection. Wet injection is convenient, but limited by the low sensitivity of samples per unit volume for Sb isotopic analysis. Hydride generation injection has the advantage of highly efficient sample transport to increase the sensitivity of Sb and thus decrease the minimum Sb concentration required. In addition, hydride generation can separate Sb from the matrix and has a higher tolerance to the matrix effect compared to the other introduction systems. To date there is no consensus on an international reference ("zero-delta"), against which can Sb isotope results be expressed. The Sb isotope measurements reported in the literature are expressed relative to different standards, making interlaboratory comparisons difficult if not impossible.

Here we report a few improvements and refinements toward high-precision measurement of Sb isotopes in environmental and geochemical samples. To improve the sample purification, we employed a two-column ion exchange set-up, including a cation-exchange resin column to remove most matrix elements, such as K, Ca, Fe, Zn, Pb, Ni, and Co in solution, followed by the use of a thiol resin column to separate the hydride-forming elements, such as Sn, Se, Ge, As, and, in particular Te, from Sb. A model that combines SSB with internal normalization of Cd was used to correct the instrument mass bias. Spectral interferences, matrix effects and concentration effects on the Sb isotope ratio determination have been carefully calibrated. Following the success of using the single-element standard reference materials (SRM) from the U.S. National Institute of Standards and Technology (NIST) for the measurement of stable isotopes such as Cd, Cr, and Hg (Abouchami et al., 2012; Schoenberg et al., 2008; Blum and Bergquist, 2007), we tested the performance of NIST SRM 3102a (Sb standard solution) as the reference standard for Sb isotopes to resolve the interlaboratory discrepancies in Sb isotope data. We then used this reference standard to normalize Sb isotopic data reported in the literature to allow interlaboratory comparisons. Using this refined approach, we were able to successfully determine high-precision Sb isotope composition of a variety of environmental and geochemical solid reference samples such as soil, sediment, coal, fly ash, plant and shale.

2. Experimental section

All laboratory work was carried out in ISO class-100 laminar flow hoods in a class-1000 ultraclean room at the State Key Laboratory of Environmental Geochemistry, Institute of Geochemistry, Chinese Academy of Sciences, in Guiyang, China.

Table 1
Existing methods of sample preparation and analysis for Sb isotope measurement. Adapted from Wen et al. (2018), Tan et al. (2020) and Ferrari et al. (2021)

Reference	Pre-concentration and separation			MC-ICP-MS analysis			Standard
	Ion exchanger	Yield (%)	Sample introduction system	Method of mass bias correction	The lowest Sb concentration	Precision (‰)	
Rouxel et al. (2003)	Biorad AG50-X8 resin and TCF	82	Hydride generation system	SSB	10 ng	0.04	SPEX
Asaoka et al. (2011)	TCF	99.5 ± 3.6	–	Sn doping	–	0.04	SPEX
Tanimizu et al. (2011)	TCF	–	Nebulizer and spray chamber	Sn doping	50 ng/ml	0.04	SPEX
Lobo et al. (2012, 2013, 2014)	Dowex AG50-X8 and Amberlite IRA 743 resins	>76	Nebulizer and spray chamber	In, SSB and RRL	200 ng/ml	0.02–0.06	SCP Science
Degryse et al. (2015)	Dowex AG50-X8 and Amberlite IRA 743resins	–	Nebulizer and spray chamber	In and SSB	200 ng/ml	0.01(RSD)	SCP Science
Resongles et al., 2015	TCP	96 ± 2	Hydride generation system	SSB	1 ng/ml	0.06	SCP Science
Liu et al. (2020)	AG -X4 and AG 50 W-X8	98.7 ± 5.6	nebulizer and spray chamber	SSB and Cd doping +SSB	200 ng/ml	0.04	NIST 3102a
Li et al. (2021)	Thiol-silica	>95.2	Desolvation system	SSB and In doping	75–100 ng/ml	0.04	SPEX
Ferrari et al. (2021)	Thiol-silica powder	100 ± 7	Hydride generation system	SSB	1 ng/ml	0.05	SPEX
This study	Biorad AG50-X8 resin and Thiol resin (Cleanert SH)	99.5 ± 4.1	Hydride generation system and Aridus II/ equipped with a 50 μL/min PFA nebulizer	SSB and Cd doping	0.5 ng/ml	<0.04	NIST 3102a

Thiol Cotton Fiber (TCF), Thiol-celluloase powder (TCP), Standard-sample bracketing method (SSB), Revised Russell's Law (RRL).

2.1. Reagents and materials

Hydrochloric, hydrofluoric, and nitric acids (ultrapure grade) from Sinopharm Chemical Reagent (China) were double-distilled with a DST-1000 acid purification system (Savillex, USA) prior to use. H_2O_2 (35%, wt./wt., guarantee reagent grade) was obtained from Thermo Fisher Scientific (USA). Potassium iodide (ACS reagent, ≥99%), L-ascorbic acid (ACS reagent, ≥99%), NaOH (ACS Reagent, >97%), and $NaBH_4$ (99%) were from Sigma-Aldrich (USA). The cation exchange resin AG50W-X8 (200–400 mesh) and 10 mL polypropylene columns were from Bio-Rad (USA). All dilutions were performed with ultra-pure water (MQ, 18.2 MΩ. cm). The PFA beakers (15 mL), pipet tips, and centrifuge tubes (7 mL) were first cleaned with MQ water, then with 50% (*v*/v) HNO_3, 10% (v/v) HNO_3, and 4 M HCl, respectively, and finally thoroughly rinsed again with MQ water, before being air-dried in an ISO class-100 hood (Zhu et al., 2018; Wu et al., 2020). Silica-based thiol resin (Cleanert SH, pore size: 60 Å, grain size: 40 μm) was from Tianjin Bonna-Agela Technologies (China). The use of commercial thiol resins improves the consistency and reproducibility of sample separation and preconcentration compared with thiol cotton fiber. The same commercial thiol resins have been used for preconcentrating Se from seawater (Chang et al., 2017). The cleaning procedure of thiol resins is as follows: an amount of thiol resin was placed in a 100 mL bottle, which was washed on a shaker for 1 h, two times with Milli-Q water, three times with 6 M HCl, and then two times with 0.5 M HCl. After cleaning thiol resins were stored inside ultra-pure water.

2.2. Reference materials

Environmental and geochemical reference materials BCR-482 (lichen) and BCR-176 (fly ash) were from European Commission - Joint Research Centre Institute for Reference Materials and Measurements, whereas GXR-1 (jasperoid), GXR-4 (copper mill-head), GXR-6 (soil), and SGR-1b (shale) were purchased from the US Geological Survey (Reston, VA, USA). Other reference materials included GSS-5, GSS-8, GSS-12, GSS-14 (soil), GBW-11108 L and GSD-3a, GSD-11, and GSD-12 (sediment) were from the Institute of Geophysical and Geochemical Exploration of the Chinese Academy of Geological Sciences, and SRMs 1633c (fly ash), 1632d (coal), and 2711a (soil) were from the NIST. All of these materials were used as test samples for Sb isotope ratio measurements. The Sb isotope analysis results of this study were reported against NIST SRM 3102a (lot: 140911). High-purity Sb solutions from Sigma-Aldrich (Merck, Germany; lot: BCBT7006), Alfa Aesar (USA; lot: 1227270B), Spex Certiprep (USA; lot: CL 10-49SBY), and SCP Science (Canada; lot: 140–051-511) were used as the secondary standard solutions with different Sb isotopic compositions.

2.3. Sample digestion

We used a series of the aforementioned reference materials to evaluate the reliability of the purification process. Typically, 50 to 100 mg of the shale, soil, sediment, or plant samples were weighed into 15 mL modified Teflon-lined (TFM) vials and digested with 3 mL mixed HNO_3-HF (HNO_3/HF = 5:1 v:v) in customized, high-pressure bombs, and heated at 185 ± 5 °C for at least 48 h. After complete digestion, the samples were dissolved in 2 M HNO_3 for Sb purification. Details of the digestion procedures can be found in Zhu et al. (2018) and Wu et al. (2020). It should be noted that the temperature of the hot plate should not exceed 90 °C when the sample solutions are evaporated into incipient dryness, due to the volatile nature of some Sb compounds.

2.4. Antimony purification

The Sb isotope separation and purification process used in the experiment was improved by combining ion exchange chromatography and thiol resin columns (Rouxel et al., 2003; Resongles et al., 2015; Yu et al., 1983; Marin et al., 2001), as shown in Table 2. Before loading the column, an appropriate volume of the sample solution (containing about 30–100 ng Sb) was placed into a 15 mL PFA beaker. 0.3 mL H_2O_2 and 0.5 mL HNO_3 were then added to convert all Sb species to Sb(V). After tightly closing its lid, the PFA cup was placed on a hot plate at 100 °C for 0.5 h, which was then opened and steamed at 90 °C until the content was almost dry. Finally, the content was dissolved in 1 mL 0.14 M HF at 90 °C for 10 min until a clear solution without any residue was achieved.

The subsequent pretreatment process in this study is divided into the following two major steps:

2.4.1. Step 1: removal of matrix elements by cationic resin exchange column

This step is to remove matrix elements, and can be skipped when preparing samples with low matrix element contents, such as most natural water samples. The 10-mL polypropylene exchange column was loaded with 2 mL AG50W-X8 cation resin (200–400 mesh) without any air bubbles. After placing the resin, the column was washed first with 6 M HCl. Subsequently, a total of 10 mL MQ water balance was added to the resin by 1 ml by 1 ml. The amount of MQ water could be increased to rinse the resin to neutrality. The sample was evaporated to near dryness, and then filled up to 1 mL with 0.14 M HF before being added to the column. The column was washed with a total of 4 mL MQ water, in 1 mL portions. Matrix elements such as K, Ca, Fe, Zn, Pb, Ni, and Co would be retained on the ion exchange column, whereas Sb would pass through the column along with fractions of elements such as Sn, Se, Ge, As, and Te. 15 mL PFA beakers were used to collect all the column solution from the sample to the MQ washing column, after which they were heated on a hot plate at 90 °C until near dryness. Note that the temperature of the hot plate should not exceed 90 °C during the drying process. There were no volatile Sb compounds when using open vessel system according to the near 100% recovery, as discussed in Section 3.3, which is consistent with the findings reported previously (Rouxel et al., 2003; Ferrari et al., 2021).

2.4.2. Step 2: pre-concentration of Sb (III) onto thiol resin column

After the eluent in step 1 was evaporated to near dryness, a 10% *w/v* KI and L-ascorbic acid mixed solution, HCl, and MQ water were added (~2 mL), and the solution medium was changed to 0.5 M HCl, 0.5% w/v (KI + L-ascorbic acid), which would convert all Sb(V) to Sb(III). Thereafter, 1.00 ± 0.01 g of thiol resin was loaded into the polypropylene exchange column. After being washed with 10 mL MQ water and 4 mL 5 M HCl, and equilibrated with 6 mL 0.5 M HCl, the reduced sample

Table 2
Two-step chromatographic Sb purification protocols used in this study.

Separation stage	Reagent	Volume (mL)
Step I		
Column I: Cation exchange resin (AG50-X8, 200–400 mesh, 2.0 ml)		
Washing	6 M HCl	10
Washing to near neutral	Milli-Q Water	10
Sample in 0.14 M HF, load and collect	0.14HF	1
Washing and collecting	Milli-Q Water	4
Step II		
Column II: Cleanert SH thiol resin (0.5–1.0 g)		
Washing	Milli-Q Water	10
Washing	6 M HCl	4
Condition	0.5 M HCl	6
Sample (Sb(III)) in 0.14 M HF, load 0.5% KI+ 0.5% L-ascorbic acid solution	load	2
Eluting Sn	2.5 M HCl	7
Collecting Sb	6 M HCl	8
To be measured after dilution to 3 M HCl medium		

solution was loaded into the column. Subsequently, the column was washed with 7 mL 2.5 M HCl. Finally, the column was washed with 8 mL 6 M HCl, and the eluent was collected in a 7 mL PFA beaker, to which the KI + L-ascorbic acid solution was added to prevent the Sb (III) from being oxidized. In this chemical preparation, the elements that formed hydrides including Sn were eluted with 2.5 M HCl. Other elements such as Sn, Se, Ge, As, and particularly Te were retained on the thiol resin columns. The reducing agent, KI, and L-ascorbic acid solution improved the separation efficiency of Sb and Te. Some of the Te was also lost via volatilization during the heating and drying processes.

The Sb-containing eluent was then diluted to 3 M HCl, and analyzed for Sb isotopes using a hydride generation system in conjunction with MC-ICP-MS.

2.5. Determination of Sb isotopic composition

A home-made hydride generation (to produce SbH_3) sample introduction system, combined with a PFA aspiration nebulizer with an uptake rate of 50 μL/min (Fig. 1), was coupled to a Nu Plasma II MC-ICP-MS (Nu Instruments Ltd., UK) for the Sb isotope ratio measurements. Typical operating conditions for the MC-ICP-MS are shown in Table 3.

The hydrides were formed by reacting Sb(III) of samples, conditioned in 3 M HCl, with freshly prepared sodium borohydride (0.5 wt% $NaBH_4$ in 0.5 wt% NaOH) (Lima et al., 2020):

$$3BH^{-}_{4(aq)} + 3H^{+}_{(aq)} + 4H_3SbO_{3(aq)} \rightarrow 3H_3BO_{3(aq)} + 4SbH_{3(aq)} + 3H_2O \quad (1)$$

The Nu Plasma II was run in the low-resolution mode, with a mass resolution of ~2000 (Table 3). Ion beams at ^{111}Cd (L4), ^{112}Cd (L3), ^{113}Cd (L2), ^{114}Cd (L1), ^{115}In (Ax), ^{120}Sn (H5), ^{121}Sb (H6), ^{123}Sb (H7), and ^{125}Te (H8) were collected simultaneously in a single cycle using Faraday cups, with all channels connected to amplifiers with 10^{11} Ω resistors. Instrumental background and acid matrix blanks were corrected by on-peak acid blank measurements carried out before every sample and standard. All samples were treated the same as the standards to account for variation in the intensity of residual interferences. The matrix interference correction is described below.

The time of sample take-up was 500 s, and the washing time was at least 300 s to lower the Sb signal to <1 mV. With an injecting

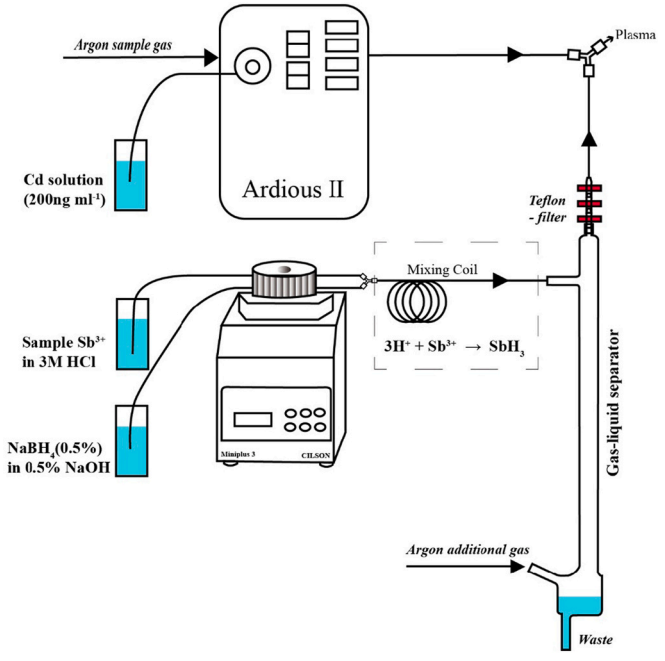

Fig. 1. An illustration of the sample introduction system for Sb isotope ratio measurements.

Table 3
Operating parameters for the HG-MC-ICPMS system.

Hydride generator	Designed and manufactured by our research group
Solution compositions	
Washing solution	3 M HCl
$NaBH_4$	0.5 wt% $NaBH_4$ in 0.5 wt% NaOH
Sample or standard acidity	3 M HCl
Mass spectrometer	Nu Plasma II MC-ICP-MS
Cup configuration	
Cup mass	L4(111), L3(112), L2(113), L1(114), Ax(115), H3(118), H6(121), H7(123), H8(125)
Operating parameters	
Introduction system (Cd)	Aridus II with a 50 μL/min PFA nebulizer
Sample cone	Nickel
Skimmer cone	Nickel
RF power	1300 W
Resolution	Low
Cooling Ar flow rate	15.0 L min^{-1}
Auxiliary Ar flow rate	0.80 L min^{-1}
Sample Ar flow rate	0.06 L min^{-1} (adjusted daily)
Nebulizer Ar flow rate	20 PSI (adjusted daily)
Sweep gas flow rate in Aridus II	1.8 L min^{-1} (adjusted daily)
Analysis	
Number	1 block of 50 cycles
Integration time	10 s
Sample transfer time	60 s
Sample washout time	300–600 s

concentration of 0.5–3 μg L^{-1}, the total amount of Sb required for each measurement was ~3.0–21 ng. The Sb isotopic composition of all the samples and standards were expressed relative to the NIST SRM 3102a in a delta or epsilon notation:

$$\delta^{123}\mathrm{Sb} = \left[\left(^{123}Sb/^{121}Sb\right)_{Sample} \Big/ \left(^{123}Sb/^{121}Sb\right)_{Standard} - 1\right] \times 1000 \quad (2)$$

$$\varepsilon^{123}\mathrm{Sb} = \left[\left(^{123}Sb/^{121}Sb\right)_{Sample} \Big/ \left(^{123}Sb/^{121}Sb\right)_{Standard} - 1\right] \times 10000 \quad (3)$$

3. Results and discussion

3.1. Mass bias correction

The mass discrimination caused by the space charge effect, ion transport efficiency, and other factors in the MC-ICP-MS instrument affects the measurement accuracy. To achieve accurate and precise Sb isotope ratio measurements, a model combining SSB (Rouxel et al., 2003) with internal normalization (element doping) (Lobo et al., 2012) (SSB-ED) was used to correct the instrument mass bias. This model can correct the short-term fluctuation of instrument, but cannot compensate the mass bias induced by the matrix.

The formula of SSB is as follows:

$$\varepsilon^{123}\mathrm{Sb} = \left\{ \frac{\left(^{123}Sb/^{121}Sb\right)_{Sample}}{\left[\left(^{123}Sb/^{121}Sb\right)_{Standard-1} + \left(^{123}Sb/^{121}Sb\right)_{Standard-2}\right]/2} - 1 \right\} \times 10000 \quad (4)$$

where $(^{123}Sb/^{121}Sb)_{Sample}$ represents the measured Sb isotope ratio of the sample, and $(^{123}Sb/^{121}Sb)_{Standard\text{-}1}$ and $(^{123}Sb/^{121}Sb)_{Standard\text{-}2}$ are the ratios in two isotopic standards.

In previous studies, Sn (Tanimizu et al., 2011; Asaoka et al., 2011) and In (Lobo et al., 2012, 2013, 2014) were used as the doping mass discrimination correction technique. However, we found an occurrence of high Sn background in the hydride generation system, but not in the direct injection with the nitric acid medium. Therefore, we did not use

Sn as an internal standard for mass bias correction when using hydride generation for sample introduction. The abundance difference between the In isotopes (91.4%) was much larger than that between the Sb isotopes (14.4%), which probably would cause the difference in the mass discrimination effect. The removal rates for In in all Certified Reference Materials (CRMs) were almost >98% and the signals of In in the purified samples analyzed by HG-MC-ICPMS were <0.001 V levels, which can be negligible.

As a result, Cd was selected as the internal normalization element in Sb isotope analysis for mass bias correction. With eight stable isotopes, i.e., ^{106}Cd (1.25%), ^{108}Cd (0.89%), ^{110}Cd (12.47%), ^{111}Cd (12.80%), ^{112}Cd (24.11%), ^{113}Cd (12.23%), ^{114}Cd (28.74%), and ^{116}Cd (7.51%), Cd is an ideal internal standard element, as its isotopic masses are close to those of Sb and without spectral interference on ^{113}Cd/^{111}Cd. The Cd isotope standard NIST SRM 3108 has been commonly used in Cd isotope research and analysis for its long-term stability (Abouchami et al., 2012; Tan et al., 2020). The mass fractionation factor obtained from the bracketing certified reference material NIST SRM 3108 (^{113}Cd/^{111}Cd = 0.95542, certified value from Abouchami et al., 2012) was used to correct the ^{121}Sb/^{123}Sb value by employing the Russell law.

In the analytical processes, the Cd standard was injected through a desolvation device sample introduction system, whereas the Sb sample was injected through the hydride generation system. After Cd and Sb aerosol mixing, they were injected together into the MC-ICP-MS plasma, with a signal ratio of 1:1. Applying the empirical method of Maréchal et al. (1999), a logarithmic linear regression for the raw isotope ratio data followed a fractionation line in the ln(^{113}Cd/^{111}Cd) vs. ln (^{123}Sb/^{121}Sb) isotope measurements (Fig. S1). The slope of 0.982 was close to the value predicted by the exponential law (Russell et al., 1978) (0.918), and thus could be used directly for correction (Lobo et al., 2012).

3.2. Spectral interferences and matrix effects

The isobaric interferences of the Sb isotope measurements were present from other elements (e.g., K, Ca, Fe, Zn, Pb, Ga, Ge) as some of their compounds have similar *m/z* values (e.g., Sn hydrides and argon dimers). The potential interferences on Sb isotopes are summarized in Fig. S2. Non-spectral mass discrimination (i.e., the matrix effect) interferences from abundant elements, such as Na, Mn, Mg, Ca, Mg, Mn, Al, Ti, and Zr, are negligible as they were efficiently removed by the cation exchange resin and thiol resin columns, with a nearly 100% separation efficiency. The matrix effect intensities measured for Sb isotopes were < 0.001 V background levels during the hydride generation process. The elution sequence was further studied by the analysis of Nist 2711a, Nist 1632d, BCR 176R, GSD-12, and BCR 482 (Fig. S3 and Table. S1). Subsequently, the matrix effects of the potential presence of Al, Cu, Fe, Se, Te, and As on Sb isotope analysis are evaluated. The presence of Al, Cu, and Se ([elements]/[Sb] up to 1000) did not affect the accuracy of Sb isotopic analyses. Generally, matrix-induced mass bias (Fe/Sb ≥ 1000 or As/Sb ≥ 100) can cause an obvious drifts ofε^{123}Sb. For iron, one cause originates from the precipitation of metal borides and another one can prevent hydride formation by oxidizing Sb (III) to Sb(VI) (Sanz et al., 1990). For arsenic (a hydride-forming element), competition with Sb for reaction with $NaBH_4$ should decrease Sb hydride formation rate (Ferrari et al., 2021).

The presence of Te in the samples could be particularly problematic for precise Sb isotope measurements due to their similar masses. In our study, Cleanert SH thiol resin was selected for the Sb samples, which resulted in effective separation of Sn and Te, with a Sb recovery rate of approximately 100%. Nevertheless, spectral interferences on Sb isotopes from Te, TeH^+, and SnH^+ were examined by doping with Te and Sn. We spiked 3 ng g^{-1} Sb NIST SRM 3102a standard solutions with various amounts of Te (0.0003–30 μg L^{-1}) or Sn (3–600 μg L^{-1}), and the Sb isotope ratio was measured against Sb NIST SRM 3102a standard to evaluate the interference and correction. The ε^{123}Sb values were found to be sensitive to Te contents in the sample solutions because ^{123}Te, and $^{122}TeH^+$ and $^{120}TeH^+$ could induce interferences on ^{123}Sb and ^{121}Sb, respectively. Te could form hydrides in the hydride generator, but the hydride generation rates were variable. The same experimental results were obtained by Wasserman and Johnson (2020) in Te isotope measurements. The Te content in the blank was negligible, so it should not influence the Sb isotopic measurements. The addition of Te significantly interfered the ratios of Sb isotopes, as shown in Fig. 2. Since the efficiencies of different hydride generating systems are different, we suggest that the signal of ^{125}Te should be kept as being less than 10^{-4} V, in order to obtain precise measurements. Even with a Sn/Sb ratio of up to 200 in the sample solutions, there was no significant influence on the Sb isotope measurements. However, interferences from Sn^{112} and Sn^{114} led to a considerable challenge to the precise measurements of ^{112}Cd and ^{114}Cd isotope (doping element), resulting in a correction fractionation coefficient error. In addition, the carrier gas of MC-ICPMS contains a small amount of Kr. There is a chance of the isobaric interference from $^{78}Kr^{36}Ar$ on ^{114}Cd. Therefore, ^{111}Cd and ^{113}Cd isotopes were used to correct the instrumental mass bias as described above.

3.3. Yields and blanks

The Sb yields of the combined sample digestion and ion-exchange columns were 101% ± 4.1% (mean ± 2 standard deviation (SD), n = 190). Statistically (t-test) no Sb isotopic fractionation (^{123}Sb < 0.4ε) was induced by the purification process. In the Sb isotope pretreatment process, from sample digestion to the final two purification separations, the total Sb procedural blank (n = 30) was generally <0.3 ng. The analyzed Sb content in the environmental samples, including sediment, soil, plant, water, dry ash, and coal, thus needs to be above 30 ng in order to limit the blank contribution to <1%, which requires isotopic fractionation either not occurring during the process or being corrected by SSB-ED (Wasserman and Johnson, 2020; Friebel et al., 2020). The total procedural blank of Sb was mainly produced in the complete separation procedure (<0.28 ng), and the digestion of the samples (<0.02 ng) only contributed a very small portion and could be ignored in this study. For low Sb content samples, we would recommend multiple digestion of the samples and mixing them before the separation and purification procedures.

3.4. Precision and accuracy

To evaluate long-term reproducibility, four high-purity Sb solutions from Sigma-Aldrich, Alfa, Spex, and SCP, in addition to the NIST SRM 3102a standard, were measured over a period of one year (Fig. 3). The long-term external reproducibility of the NIST SRM 3102a standard by our analytical routine was estimated conservatively to be better than 0.4ε, comparable to that reported by Rouxel et al. (2003), Tanimizu et al. (2011), and Asaoka et al. (2011). Using NIST SRM 3102a as the reference standard, ε^{123}Sb values of 1.00 ± 0.36 (n = 31, 2SD), 2.83 ± 0.39 (n = 85, 2SD), 3.76 ± 0.31 (n = 29, 2SD), and 3.01 ± 0.18 (n = 7, 2SD) were obtained for the Sigma-Aldrich, Alfa, Spex, and SCP Sb solutions, respectively, over the one-year period (Fig. 4), all with a long-term precision better than ±0.4ε. In order to obtain the minimum sample content loading for Sb stable isotopes analysis, the Alfa Sb solutions, at Sb concentrations of 0.2, 0.5, 1, 1.5, 2, 3, and 5 μg L^{-1}, were measured repeatedly to further evaluate the precision at different sample concentrations (Fig. 4). The 2SD precision of the Alfa Sb was consistent with the long-term reproducibility, and the average values were all within the error margin (0.4ε). High-precision (2SD ≤ 0.5ε) and accurate Sb isotope composition could be determined by our method at concentrations as low as 0.5 μg L^{-1} Sb. To further test the uniformity of the NIST 3102a standard, two different bottles of the standard solution that were purchased separately were used in this study and in [35] Liu et al. (2020) for the Sb isotope measurements of GSS-5, GSD-11, and the Alfa Sb solution. As shown in Fig. S4, our ε^{123}Sb values agree very well with

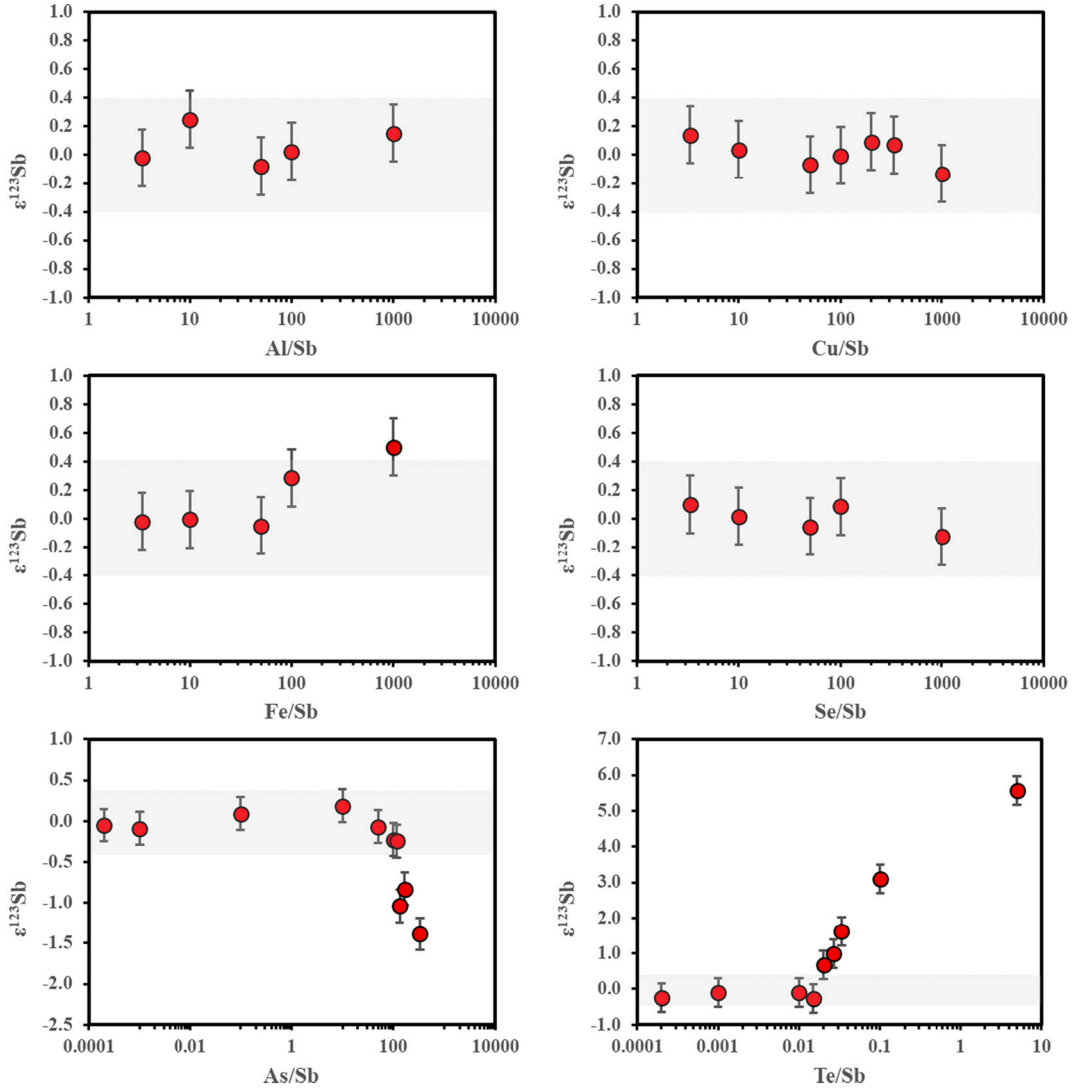

Fig. 2. The effects of different elements with varying [element]/[Cd] on the ε^{123}Sb values measured at 3 ng/ ml for Nist 3102a. The gray band denotes the long term external precision (±0.4ε, 2SD).

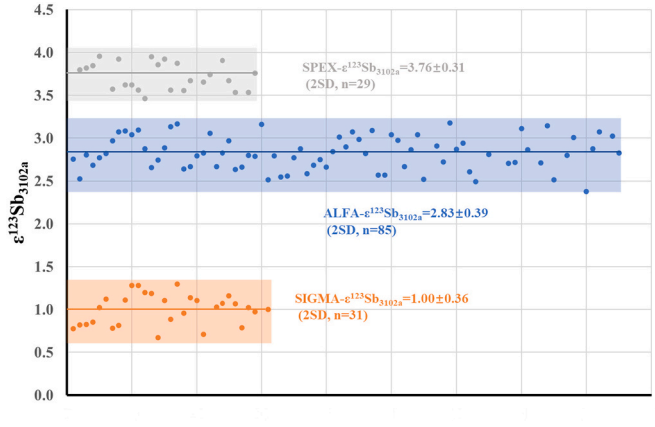

Fig. 3. Precision and accuracy of the SSB-ED mass bias correction models for the Sb isotope ratio in the Alfa, Sigma, and Spex Sb in-house standards relative to the bracketing standard of NIST SRM 3102a over a period of six months. The horizontal line represents the mean ε^{123}Sb value. The gray area represents error +/− 2SD of the ε^{123}Sb value.

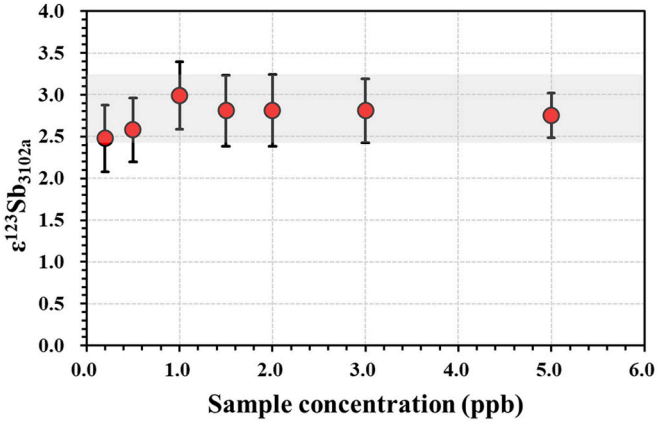

Fig. 4. A comparison of measured Sb isotope results for NIST SRM 3102a at varying Sb concentrations.

the results reported by Liu et al. (2020), suggesting a high Sb isotope uniformity in the NIST standard. Furthermore, in order to confirm the accuracy and precision of Sb isotope measurement on purified and

measurement protocol, three standard addition experiments were carried out, including 1) spiking NIST 3102a to the Spex Sb solution, 2) spiking NIST 3102a to GSS-5 followed by the purification procedure; and 3) spiking NIST 3102a to NIST 1632d followed by the purification procedure. A linear regression curve between ε^{123}Sb and the Sb fraction was obtained, with $R^2 > 0.988$, in all the standard addition experiments (Fig. S5), further supporting the accuracy of the proposed method.

3.5. Concentration effect on the Sb isotope ratios determination

To evaluate the concentration effect on the Sb isotopic determination (i.e., to test whether the instrument's mass bias changes with the Sb concentration to be measured in the samples), a series of solutions with the Sb concentration ranging from 0.08 to12 times of the standard solution were prepared and analyzed for Sb isotopic ratios relative to the standard solution. As shown in Fig. S6, even within such a large concentration matching rate range, the concentration effect on the determination of Sb isotopes was negligible. This suggests that the SSB-ED method used in this study is highly effective. Other important factors include the high sensitivity of our instrument, the high efficiency of the Sb hydride reaction in the solutions, and the stable ICP ionization efficiency. However, the function of the sample/standard ratio approximate one was suggested, because if the very last data point was removed, it looks as if there is a trend in the Sb isotopic composition as a function of the sample/standard ratio.

3.6. Antimony isotopic composition of environmental reference materials

The Sb isotope composition in environmental reference materials are shown in Table S2. The sample types were chosen intentionally to span a range of matrix types to be representative of various environmental samples. The sample types included plant (BCR-482), shale (SGR-1b), sediment (GSD series), soil (GSS series), coal, and fly ash (NIST-1633c, BCR-176R). At least ten replicates of each sample were digested and purified following the new approach. The corrected values were obtained based on the ratio of $^{111}Cd/^{113}Cd_{Nist\text{-}3108}$ and, subsequently, calculated by using a combination of calibrator-sample bracketing and internal normalization. As shown in Fig. 5, the ε^{123}Sb values of these environmental reference materials range from 0.29ε to 5.36ε, with a large span of 5.07ε. As the Sn/Sb, In/Sb, and Te/Sb concentration ratios in the purified reference sample solutions were <0.005, the spectral interference of polyatomic ions (e.g., $^{120}SnH^+$, $^{120}TeH^+$, $^{122}SnH^+$, ^{113}In, $^{112}SnH^+$) are negligible. These results support that our method is suitable for a variety of sample matrices.

3.7. Comparison of Sb isotope ratios between different laboratories

To allow interlaboratory comparisons, we normalized all the literature data relative to NIST SRM 3102a (Fig. 6) based on the following equation (Feng et al., 2019).

$$\delta_{A,C} \approx \delta_{A,B} + \delta_{B,C} \quad (5)$$

where A, B, and C are three different reference materials.

The ε^{123}Sb values of BCR 176, GXR-4, and NIST 1643e in our study and in the literature (Rouxel et al., 2003; Resongles et al., 2015) were used to transform as the basic references. The NIST 1643e was prepared from the same material as the NIST SRM 3100 series of single-element solutions. Consequently, the compositions of NIST SRM 3102a and 1643e are considered to be the same. The results show that plant, soils, coal, rock, sediments, fly ash, and water have substantial ε^{123}Sb variations over a range of about 19.3ε, being enriched in or lacked of Sb isotope relative to NIST SRM 3102a. Together with the indication that strong fractionation (9ε) occurs during Sb(V) reduction to Sb(III) (Rouxel et al., 2003), our results support the use of Sb isotope fractionation as a promising tool to distinguish natural and anthropogenic

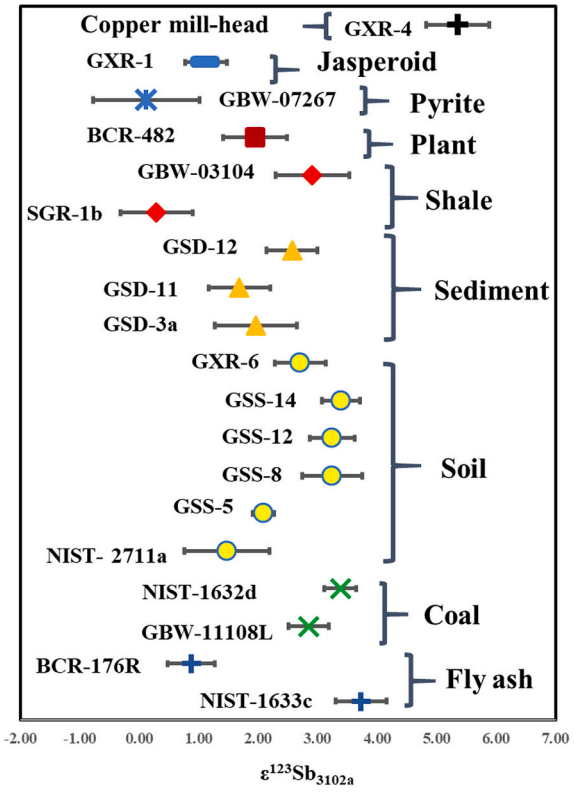

Fig. 5. ε^{123}Sb values in selected environmental reference materials measured by this study.

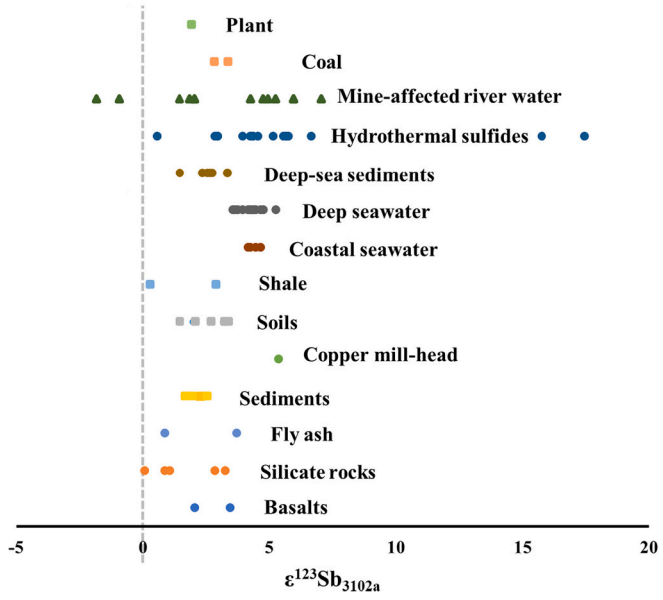

Fig. 6. Antimony isotopic composition of different environmental, geological and anthropogenic materials. The data are compiled from Rouxel et al. (2003) (circles) and Resongles et al. (2015) (triangles), and reported in this study (squares).

sources and processes of Sb in the environment such as remobilization, oxidation, reduction, and deposition. To understand Sb cycle in surface environment, quantifying the Sb isotopic compositions in different pools such like soils, sediments and seawater are one of critical approaches. The mean ε^{123}Sb is 2.69 ± 0.77 (1σ) for soils, 2.07 ± 0.45 (1σ) for steam sediments, 2.66 ± 0.65 (1σ) for deep-sea sediments, 4.28 ± 0.47 (1σ) for

deep seawater, and 4.40 ± 0.40 (1σ) for coastal seawater. The relatively positive values of Sb isotopic composition in soils than that in sediment may be explained by Sb from different sources and processes. The Sb isotopic composition of deep-sea sediments are negative than those of deep and coastal seawater, which requires further study about Sb sources and sinks of oceanic system (Rouxel et al., 2003). The ε^{123}Sb values in igneous basalt rocks, other silicate rocks and shale are presented to be 2.77 ± 0.99 (1σ), 1.63 ± 1.37 (1σ) and 2.02 ± 1.50 (1σ), respectively, which are similar to those of soils and sediments. The differences are significant for plant (BCR 482) and coal (Nist 1632d and GBW-coal), suggesting potential influences of vegetal species and coal forming processes on the ε^{123}Sb signature.

4. Conclusions

We presented a highly accurate and precise method to determine Sb isotope composition in environmental and geochemical samples. This method involves a two-column separation of matrices and hydride generation before MC-ICP-MS measurements and employs an SSB-ED mass bias correction approach with Cd as the internal standard element. The method blank is <0.3 ng of Sb, and the overall sensitivity is~2 V per ppb of Sb, making it possible to measure Sb isotopes with samples containing as low as 3.0 ng of Sb. This minimum Sb content could be further lowered with additional improvement in the total blank and digestion procedures of large mass samples. We have also shown the long-term stability (0.4ε) and uniformity of Sb isotope composition in NIST SRM 3102a, making it an ideal reference standard for Sb isotope measurements to resolve the interlaboratory discrepancies in Sb isotope data.

The advances of this method compared to existing ones are in the following aspects. Firstly, hydride generation with internal normalization of Cd was used to analyze Sb isotopic composition, which has the advantage of correcting the short-term fluctuations in mass bias between bracketing standards compared to the direct SSB. Secondly, a minimum Sb of as low as 3.0 ng required per analysis was achieved by the hydride generation used. Thirdly, thiol resin was successfully applied to the separation of Sb from complex solid matrices with a low Sb content, and the advantage of using thiol resin instead of traditional thiol cotton is to abandon the use of a large number of toxic substances and greatly improve the repeatability of operation. Fourthly, a large number of reference materials were reported and a standard reference material certified for the total Sb concentration, NIST SRM 3102a, which is also recommended for Sb isotope measurements, providing the possibility for interlaboratory comparison. Lastly, by expressing our data and previously reported literature data against the same reference standard (NIST SRM 3102a), we provided an update on isotopic compositions of various types of environmental, geological and anthropogenic materials, which greatly improves the current understanding of Sb isotopic composition in nature. The method developed in this study provides a useful tool for future studies of Sb isotopic fractionation in various environmental conditions.

Declaration of Competing Interest

The authors declare that they have no known competing financial interests or personal relationships that could have appeared to influence the work reported in this paper.

Acknowledgments

This study was funded by the National Science Foundation of China (grant nos. 41907286), China Postdoctoral Science Foundation (2020T130649, 2018M640939), and the K.C. Wong Education Foundation. We greatly acknowledge Professor Jianming Zhu, Dr. Heng Yao, and Engineers Jing Wang, Li Zeng, and Yang Tang for their assistance in establishing the experimental method.

Appendix A. Supplementary data

Supplementary data to this article can be found online at https://doi.org/10.1016/j.chemgeo.2021.120459.

References

Abouchami, W., Galer, S.J.G., Horner, T.J., Rehkamper, M., et al., 2012. A common reference material for cadmium isotope studies—NIST SRM 3108. Geostand. Geoanal. Res. 37, 5–17.

Alvarez-Ayuso, E., Otones, V., Murciego, A., Garcia-Sanchez, A., Santa Regina, I., 2013. Mobility and phytoavailability of antimony in an area impacted by a former stibnite mine exploitation. Sci. Total Environ. 2013 (449), 260–268.

Asaoka, S., Takahashi, Y., Tanimizu, M., 2011. Preconcentration method of antimony using modified thiol cotton fiber for isotopic analyses of antimony in natural samples. Anal. Sci. 27, 25–28.

Aston, F.W., 1923. The mass-spectra of chemical elements. Phlosophical Magaz. 45 (269), 934–945.

Blum, J.D., Bergquist, B.A., 2007. Reporting of variations in the natural isotopic composition of mercury. Anal. Bioanal. Chem. 388 (2), 353–359. https://doi.org/10.1007/s00216-007-1236-9.

Chang, Yan, Zhang, Jing, Qu, Jian-Quo, Xue, Yun, 2017. Precise selenicum isotope measurement in seawater by carbon-containing hydride generation-Desolvation-MC-ICP-MS after thiol resin preconcentration. Chemical Geology 471, 65–73. https://doi.org/10.1016/j.chemgeo.2017.09.011. In this issue.

Degryse, P., Lobo, L., Shortand, A., Vanhaecke, F., Blomme, A., Painter, J., Gimeno, D., Eremin, K., Greene, J., Kirk, S., Walton, M., 2015. Isotopic investigation into the raw materials of late Bronze Age glass making. J. Archaeol. Sci. 2015 (62), 153e160.

Dupont, D., Arnout, S., Jones, P.T., Binnemans, K., 2016. Antimony recovery from end-of-life products and industrial process residues: a critical review. J. Sustain. Metall. 2, 79–103.

European Commission, 2017. Communication from the Commission to the European Parliament, the Council, the European Economic and Social Committee and the Committee of the Regions on the 2017 List of Critical Raw Materials for the EU. COM, 490 Final, Brussels.

Feng, L.P., Zhou, L., Liu, J.H., Hu, Z.C., Liu, Y.S., 2019. Determination of Gallium isotopic compositions in reference materials. Geostand. Geoanal. Res. 43 (4), 701–714.

Ferrari, C., Resongles, E., Freydier, R., Casiot, C., 2021. A single-step purification method for the precise determination of the antimony isotopic composition of environmental, geological and biological samples by HG-MC-ICP-MS. J. Anal. At. Spectrom. 36, 776.

Filella, M., Belzile, N., Chen, Y.-W., 2002a. Antimony in the environment: a review focused on natural waters: I. Occurrence. Earth-Sci. Rev. 2002 (57), 125e176.

Filella, M., Belzile, N., Chen, Y.-W., 2002b. Antimony in the environment: a review focused on natural waters: II. Relevant solution chemistry. Earth-Sci. Rev. 2002 (59), 265e285.

Filella, M., Belzile, N., Lett, M.-C., 2007. Antimony in the environment: a review focused on natural waters. III. Microbiota relevant interactions. Earth-Sci. Rev. 2007 (80), 195e217.

Friebel, M., Toth, E.R., Fehr, M.A., Schonboachler, M., 2020. Efficient separation and high-precision analyses of tin and cadmium isotopes in geological materials. J. Anal. At. Spectrom. 35, 273.

Gabrielli, P., Wegner, A., Sierra-Hernández, M.R., Beaudon, E., et al., 2020. Early atmospheric contamination on the top of the Himalayas since the onset of the European Industrial Revolution. Proc. Natl. Acad. Sci. U. S. A. 117 (8), 3967–3973.

He, M.C., Wang, N.N., Long, X.J., Zhang, C.J., et al., 2019. Antimony speciation in the environment: recent advances in understanding the biogeochemical processes and ecological effects. J. Environ. Sci. 75, 14–39.

Henckens, M.L.C.M., Driessen, P.P.J., Worrell, E., 2016. How can we adapt to geological scarcity of antimony? Investigation of antimony's substitutability and of other measures to achieve a sustainable use. Resour. Conserv. Recycl. 108, 54–62.

Krachler, M., Zheng, J., Koerner, R., Zdanowicz, C., Fisher, D., Shotyk, W., 2005. Increasing atmospheric antimony contamination in the northern hemisphere: snow and ice evidence from Devon Island, Arctic Canada. J. Environ. Monit. 2005 (7), 1169–1176.

Li, S.Y., Deng, Y.L., Zheng, H.T., Liu, X., Tang, P., Zhou, J.W., Zhu, Z.L., 2021. A new purification method based on a thiol silica column for high precision antimony isotope measurements. J. Anal. At. Spectrom. 36, 157.

Lima, E.A., Cunha, F.A.S., Junior, M.M.S., Lyra, W.S., et al., 2020. A fast and sensitive flow-batch method with hydride generating and atomic fluorescence spectrometric detection for automated inorganic antimony speciation in waters. Talanta 207, 119834.

Liu, J.F., Chen, J.B., Zhang, T., et al., 2020. Chromatographic purification of antimony for accurate isotope analysis by MC-ICP-MS. J. Anal. At. Spectrom. 35, 1360.

Lobo, L., Devulder, V., Degryse, P., Vanhaecke, F., 2012. Investigation of natural isotopic variation of Sb in stibnite ores via multi-collector ICP-mass spectrometry - perspectives for Sb isotopic analysis of Roman glass. J. Anal. Atomic Spectrom. 2012 (27), 1304–1310.

Lobo, L., Degryse, P., Shortland, A., Vanhaecke, F., 2013. Isotopic analysis of antimony using multi-collector ICP-mass spectrometry for provenance determination of Roman glass. J. Anal. Atomic Spectrom. 2013 (28), 1213–1219.

Lobo, L., Degryse, P., Shortland, A., Eremin, K., Vanhaecke, F., 2014. Copper and antimony isotopic analysis via multi-collector ICP-mass spectrometry for provenancing ancient glass. J. Anal. Atomic Spectrom. 2014 (29), 58–64.
Maréchal, C.N., Telouk, P., Albarede, F., 1999. Precise analysis of copper and zinc isotopic compositions by plasma-source mass spectrometry. Chem. Geol. 156, 251–273.
Marin, L., Lhomme, J., Carignan, J., 2001. Determination of selenium concentration in sixty five reference materials for geochemical analysis by GFAAS after separation with thiol cotton. Geostand. Newslett. 2001 (25), 317–324.
Multani, R.S., Feldmann, T., Demopoulos, G.P., 2016. Antimony in the metallurgical industry: a review of its chemistry and environmental stabilization options. Hydrometallurgy 2016 (164), 141e153.
Resongles, E., Freydier, R., Casiot, C., Viers, J., Chmeleff, J., Elbaz-Poulichet, F., 2015. Antimony isotopic composition in river waters affected by ancient mining activity. Talanta 2015 (144), 851e861.
Rouxel, O., Ludden, J., Fouquet, Y., 2003. Antimony isotope variations in natural systems and implications for their use as geochemical tracers. Chem. Geol. 2003, 25e40.
Russell, W.A., Papanastassiou, D.A., Tombrello, T.A., 1978. Ca Isotope Fractionation on Earth and Other Solar-System. Materials. 42 (8), 251–273.
Sanz, J., Martinez, M.T., Galban, J., Castillo, J.R., 1990. Study of the interference of iron and mercury in the determination of antimony by hydride generation atomic-absorption spectrometry use of speciation models. J. Anal. At. Spectrom. 5 (7), 651–655.
Schoenberg, R., Zink, S., Staubwasser, M., Blanckenburg, F.V., 2008. The stable Cr isotope inventory of solid Earth reservoirs determined by double spike MC-ICP-MS. Chem. Geol. 249, 294–306.
Shotyk, W., Chen, B., Krachler, M., 2005. Lithogenic, oceanic and anthropogenic sources of atmospheric Sb to a maritime blanket bog, Myrarnar, Faroe Islands. J. Environ. Monit. 7, 1148–1154.
Smichowski, P., 2008. Antimony in the environment as a global pollutant: a review on analytical methodologies for its determination in atmospheric aerosols. Talanta 75, 2–14.
Survey, U.S.G., 2020. Mineral Commodity Summaries 2019. U.S. Department of the Interior. U.S. Geological Survey, p. 22.
Tan, D.C., Zhu, J.M., Wang, X.L., Han, G.L., Lu, Z., Xu, W.P., 2020. High-sensitivity determination of Cd isotopes in low-Cd geological samples by double spike MCICP-MS. J. Anal. At. Spectrom. https://doi.org/10.1039/c9ja00397e.
Tanimizu, M., Araki, Y., Asaka, S., Takahashi, Y., 2011. Determination of natural isotopic variation in antimony using inductively coupled plasma mass spectrometry for an uncertainty estimation of the standard atomic weight of antimony. Geochem. J. 2011 (45), 27e32.
US Office of the Secretary of the Department of the Interior, 2018. Final List of Critical Minerals, p. 23295. Federal Register 83 (No. 97).
Wasserman, N.L., Johnson, T.M., 2020. Measurements of mass-dependent Te isotopic variation by hydride generation MC-ICP-MS. J. Anal. At. Spectrom. 35, 307.
Wen, B., Zhou, J.W., Zhou, A.G., Liu, C.F., Li, L.G., 2018. A review of antimony (Sb) isotopes analytical methods and application in environmental systems. Int. Biodeterior. Biodegrad. 128, 109–116.
Wu, G.L., Zhu, J.M., Wang, X.L., Johnson, T.M., Han, G.L., 2020. High-sensitivity measurement of Cr isotopes by double spike MCICP-MS at the 10 ng level. Anal. Chem. 92, 1463–1469.
Yu, M.-Q., Liu, G.-Q., Jin, Q., 1983. Determination of trace arsenic, antimony, selenium and tellurium in various oxidation states in water by hydride generation and atomic-absorption spectrophotometry after enrichment and separation with thiol cotton. Talanta 1983 (30), 265–270.
Zhu, J.M., Wu, G.L., Wang, X.L., Han, G.L., Zhang, L.X., 2018. An improved method of Cr purification for high precision measurement of Cr isotopes by double spike MC-ICP-MS. J. Anal. At. Spectrom. 33, 809.